Polymerization-Induced Phase Separation. 2. Morphology of Polymer-Dispersed Liquid Crystal Thin Films

C. Serbutoviez,† J. G. Kloosterboer,* H. M. J. Boots, and F. J. Touwslager

Philips Research Laboratories, Professor Holstlaan 4, 5656 AA Eindhoven, The Netherlands

Received February 22, 1996; Revised Manuscript Received August 12, 1996[⊗]

ABSTRACT: Phase separation in a polymerizing diacrylate/LC mixture is shown to be driven by liquid−gel demixing rather than by liquid−liquid demixing. The structure of the gel strongly influences the initial morphology: "early" phase separation (at low conversion) produces spherical domains, whereas "late" phase separation (at high conversion) produces nonspherical domains. The higher the conversion at phase separation, the smaller the domains. A new method, simultaneous photo DSC/turbidity measurement, provides the conversion at the appearance of a nematic phase, and optical microscopy shows the development of morphology. A nonspherical droplet shape reflects the inhomogeneous structure of the polymer network. The dependence of the initial morphology on the LC content, temperature of the reaction, and cross-linker content can be explained using conversion−phase diagrams obtained from the Flory−Huggins−Dušek theory.[1] The observable part of the demixing process in a model system composed of 4-*n*-pentyl-4′-cyanobiphenyl (K15) and tetraethylene glycol diacrylate (TEGDA) probably proceeds through nucleation and growth rather than through spinodal decomposition. The phase diagram of the unpolymerized monomer/LC mixture is also reported.

1. Introduction

Polymer-dispersed liquid crystals (PDLCs) are thin films composed of microdroplets of liquid crystalline material in a polymer matrix. They can be electrically switched between a strongly scattering "off" state and a highly transparent "on" state. Therefore, they are of potential use in electro-optical devices.[2−4] One way to prepare these films is polymerization-induced phase separation which occurs when a homogeneous mixture of monomers and liquid crystals (LC) is polymerized. A preferred method is UV-induced polymerization since the curing temperature and the rate of polymerization can be chosen independently. This allows a better control of morphology. The switching properties of these materials depend strongly on a variety of parameters such as UV intensity, LC concentration, curing temperature, cross-link density, etc.[2,4−12] Morphology is considered to be a key parameter for the electro-optical behavior of such materials.[4−12] Much work has been done to optimize the switching properties, to get a high contrast at a low switching voltage, a high switching speed, and a low hysteresis.[2,4,6−9,13−15] This is very difficult, not only because of the large number of parameters involved but also due to the large number of components: practical systems usually contain a mixture of many different LC compounds and several monomers and oligomers.[4,13,16,17] We have simplified the problem by choosing a model system which consists of only one liquid crystal and one monomer. The LC is 4-*n*-pentyl-4′-cyanobiphenyl (K15) and the monomer is tetraethylene glycol diacrylate (TEGDA). Structures are given in Figure 1. By studying this simple model system, we hope to get insight into the factors which govern the phase separation process and the development of the morphology during photopolymerization. This serves as a basis for a further study of the relation between polymerization conditions and electro-optical properties in a technical system since the model system cannot be expected to exhibit optimal switching behavior.[18]

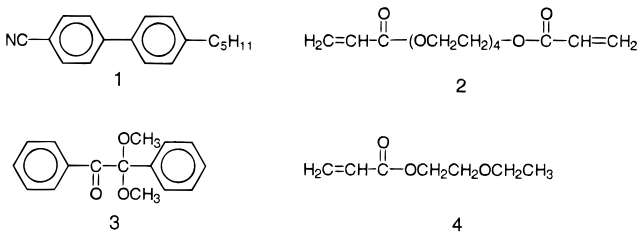

Figure 1. (**1**) K15, (**2**) TEGDA, (**3**) DMPA, (**4**) EEA.

Up to now an important driving force of the phase separation in PDLC systems has been neglected, namely the cross-linking of the polymer during reaction. Conventionally, it is assumed that phase separation occurs as a result of the increasing size of the growing polymer molecules, i.e. by liquid−liquid demixing.[3,19−22] The resulting morphology is thought to be stabilized by gelation.[3,9] This is probably correct for cross-linking polymerization through step reactions but chain reactions as used in UV-induced polymerization are characterized by gelation at low conversion, so gelation may well precede phase separation. In theoretical studies one usually starts with the phase diagram of the monomer−LC mixture and then the effect of the addition of a linear polymer is modeled.[13,19,20] In chain cross-linking polymerization not only the amount of polymer changes with conversion but also its cross-link density. This means that the phase diagram of the ternary monomer−polymer−LC system changes continuously. Theoretically, this can be visualized in a conversion−phase diagram;[1] experimentally, it means that it is very important when in the chemical reaction, at which conversion and cross-link density, the phase separation sets in. Therefore we have designed a new experimental technique which enables the measurement of the rate and conversion of the reaction as well as the simultaneous monitoring of the turbidity of the sample: photo DSC/turbidity.[23,24] This method yields the double bond conversion at incipient turbidity, i.e. the appearance of a nematic phase. A limitation of the photo DSC/turbidity method is that only conversion is determined, not cross-link density. Nevertheless, the new technique

* To whom correspondence should be addressed.

† Present address: Thomson LCD, Sextant Avionique, Z.I. Centr. Alp., 38430 Moirans, France.

⊗ Abstract published in *Advance ACS Abstracts,* October 15, 1996.

S0024-9297(96)00293-8 CCC: $12.00 © 1996 American Chemical Society

enables us to establish the importance of the gel content on phase separation and morphology. Development of morphology is studied independently using light microscopy. We have varied the LC content, the reaction temperature, and the cross-linker content of the monomer fraction. Unexpectedly, coalescence almost never occurs. This points to gelation before phase separation in most cases, i.e. to liquid−gel demixing. Also unexpectedly, rather abrupt changes in the initial size and shape of the LC domains occur upon small changes in temperature or composition. These changes can be readily explained on account of the inhomogeneous structure of the network and the shape of the conversion−phase diagram, assuming that gelation precedes phase separation. The validity of this assumption is discussed in detail. Finally, the mechanism of phase separation is briefly discussed.

2. Experimental Section

2.1. Chemicals. Tetraethylene glycol diacrylate (TEGDA) was obtained from Polysciences, 2-ethoxyethyl acrylate (EEA) was purchased from Aldrich. Monomers were used without further purification. Dimethoxyphenylacetophenone (DMPA or Irgacure 651), used as photoinitiator was obtained from Ciba Geigy. K15 (4-*n*-pentyl-4′-cyanobiphenyl) was obtained from Merck (Poole, U.K.).

2.2. Choice of Model System. In technical systems mixtures of many LC compounds are used. Since different LC compounds have different solubilities in the polymer matrix,[16] the composition of LC in droplets will be different from that of the initial LC mixture. In order to avoid such compositional changes we have chosen a very simple model system: K15/TEGDA. The monomer contains 3−4% of a photoinitiator (DMPA, Figure 1). The starting components are well-defined pure compounds, and the thermodynamics and the kinetics of the polymerization of TEGDA and other diacrylates are well-known.[25−28]

2.3. Phase Diagram before Polymerization. The phase diagram of the model system TEGDA/K15 was determined by microscopy.

The various mixtures were heated above their clearing temperature, then one drop was sandwiched between two glass plates containing fiber glass spacers with a thickness of 18 μm and next they were mounted on a heating/cooling stage (Linkam THMS 92/TMS 600) of a polarizing microscope. The light from the lamp of the microscope was filtered with a Kapton foil to avoid unwanted exposure to UV. The sample was heated above its clearing point, cooled, and observed under the microscope till crystallization occurred (magnification used: 200×) and then heated back to its clearing point. Heating and cooling rates were varied between 10 and 5 °C /min during each scan, the lowest rate being used near the phase transition.

2.4. Photopolymerization under the Microscope. The samples were prepared in the same way as those used for the determination of the phase diagram. They were cured by radiation from an Efos Ultracure 100 light source equipped with an optical fiber. The UV intensities were measured at the sample surface at a wavelength of 365 nm. UV intensities were generally low (0.1−1 mW/cm^2) in order to bring the rate of phase separation in an easily accessible time domain. The UV irradiation was stopped at the onset of the phase separation and the behavior of the droplets was examined. The samples were then cooled at 1 °C/min during 5 min and then heated back to their original curing temperature. When phase separation sets in during polymerization, a frontlike formation of droplets occurs due to the unavoidable intensity gradient in our setup. If coalescence occurs, it shows up on the video recordings made routinely during the experiments. Observations were made using a standard magnification of 200×. The resolution on the video screen is then about 1 μm . In one case (80% K15/20% TEGDA) a high-speed video was made during exposure at 7 mW/cm^2 (Kodak Ektapro EM). The sampling rate was 500 frames/s. The high-speed camera reduced the resolution. At the sampling rate chosen the time interval of observation was about 3 s. No significant differences were noticed; in particular no coalescence was observed.

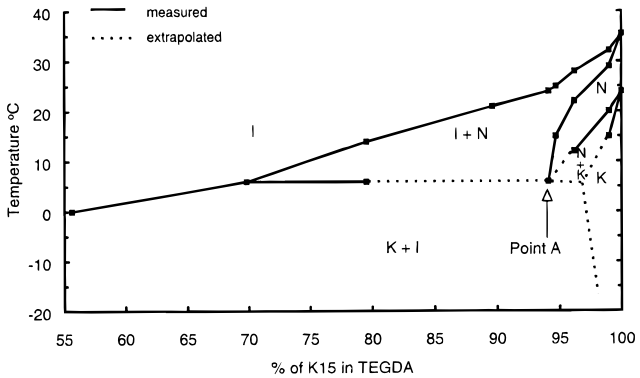

Figure 2. Binary phase diagram of K15/TEGDA obtained upon heating: I, isotropic; N, nematic; K, crystalline.

2.5. Photopolymerization in the DSC. Samples were made by sandwiching a droplet between a polished silicon disk and a glass disk of 7 mm diameter. Spacers of 18 μm were used for thickness control. Light intensities were varied between 0.08 and 8 mW/cm^2. The DSC measures the exothermic heat flux of the polymerization reaction which is proportional to the rate of reaction. Integration yields the heat of reaction; division by the total heat of reaction gives the double bond conversion, assuming complete conversion. At room temperature conversions of 90% are obtained in bulk TEGDA; in the presence of excess solvent the polymerization basically runs to completion. The DSC has been modified to monitor the intensity of a HeNe laser beam which is reflected at the bottom of the sample. When the sample gets turbid due to nematic phase formation, the intensity of the reflected light beam drops considerably. The DSC curve enables the calculation of the conversion at which turbidity sets in. The formation of isotropic droplets cannot be observed with the thin samples used. Further details have been given elsewhere.[23,24]

3. Results

3.1. Binary Phase Diagram before Polymerization. Before polymerization-induced phase separation is studied, the phase behavior of the unpolymerized model system should be established since it gives the thermodynamic stability of the starting mixture as a function of temperature and composition. Although K15/TEGDA/DMPA is a three-component system, we will treat it as a binary system assuming that the quantity of initiator always remains small with respect to the amount of LC and monomer and that its concentration remains basically constant during polymerization. The phases observed upon cooling and subsequent heating of mixtures of K15 and TEGDA are represented in Figure 2. The diagram obtained on cooling from the isotropic state is similar, albeit that the phase transition curves are shifted to lower temperatures due to super-

cooling. Three single phases, isotropic (I), nematic (N), and crystalline (K), and three biphasic regions, I + N, K + I, and N + K, can be identified. The I → I + N → N transitions can be easily and reproducibly observed. However, the temperatures at which the phase transitions N → N + K and N+I → K + I occur are difficult to measure precisely due to the formation of a supercooled nematic phase. On heating, only part of these phase transition temperatures could be measured. The dashed lines and curves represent the extrapolated position of these transitions in accord with the phase rule. On account of the existence of the transitions I + K → I + N and I + K → N + K, an invariant point A, where three phases (N, K, I) coexist, must be present. The precise position of this point could not be established but it could be estimated since A should be necessarily at the end of the phase transition curve which delimits the N phase and the I + N region.

3.2. Polymerization-Induced Phase Separation and Morphology. The onset of phase separation shows up as a frontlike formation of droplets due to the unavoidable intensity gradient under our microscope. For clarity, pictures have mainly been taken near this front. Farther in the sample or later in time the droplet density increases considerably without causing coalescence. In the limited depth resolution of our microscope a spaghetti-like structure develops toward the end of the process in most cases. Pictures of that structure are less informative than the ones obtained near the front. If coalescence occurs, it shows up on the video. We have studied the influence of LC content, temperature of polymerization, and cross-link density on the morphology. We have also determined the conversion at incipient phase separation.

3.2.1. Variation of LC Concentration and Temperature. Microscopic observations of the phase separation processes are summarized in Table 1.

A first series of experiments was carried out at high LC concentrations (90−95%). These mixtures appear homogeneous and isotropic at 20 °C, but they are thermodynamically unstable (Figure 2). Upon photopolymerization at 20 or 25 °C, spherical isotropic droplets appear at the onset of the phase separation. When observed under crossed polarizers the first droplets may show up as white spots which disappear and re-appear again at the same spot at a later time. This points to isotropic to nematic transitions and vice versa, presumably through local consumption of monomer and subsequent replenishment from the surroundings. At 20 °C some coalescence is observed; at 25 °C no coalescence is seen. The dispersions are stable in time for at least 5 min if the UV radiation is switched off and the temperature is kept constant. Slow cooling at 1 °C/min of the sample cured at 25 °C leads to an increase in size of the droplets caused by a decrease of the swelling capacity of the polymer network. The droplets soon become larger than the cell gap. As the LC domains continue to grow, their shape becomes deformed, a honeycomb-like structure develops and coalescence occurs (Figure 3). During further cooling, the droplets become nematic. Finally, the nematic phase covers the sample entirely and typical Schlieren structures, containing optically anisotropic polymeric walls, can be observed. Upon heating, the polymer walls become isotropic and next an isotropic phase develops in the LC domains. At the original curing temperature of 25 °C, the sample mainly consists of large isotropic domains separated by isotropic polymer walls.

A second series of experiments has been carried out at intermediate LC concentrations (75% to 85%). At 25 °C and 85% LC the droplets formed are spherical and nematic, right from their first appearance. If the LC content drops below 83% deformed droplets are formed. If the samples are cured at 20 °C, a similar change in shape of the LC domains from spherical to nonspherical occurs but now the transition occurs at 80% LC. At 10 °C the transition in shape is located at 77% LC. No coalescence is observed. A typical spherical morphology is shown in Figure 4. A nonspherical droplet shape may be preceded by a spherical one: for mixtures containing 80% LC or less and cured at 20 °C the LC separates out as spherical nematic droplets, but as they expand their size, their shape rapidly becomes nonspherical. The shape of the LC domains becomes more and more deformed as the concentration of LC in the starting mixtures decreases while the radiation dose to obtain phase separation increases. A typical nonspherical morphology is shown in Figure 5. Cooling after exposure of a mixture containing 85% of K15 and cured at 25 °C leads to the formation of many new small spherical droplets while the pre-existing droplets increase in size and finally become nonspherical. The largest LC domains which have a size larger than the cell gap appear black under crossed polarizers, presumably due to homeotropic alignment of the LC molecules. As in the case of high concentrations of K15, the walls around the droplets are anisotropic. By heating the sample back to its curing temperature, the newly formed droplets disappear and the size of the large deformed LC droplets decreases to nearly their original spherical shape and size. Cooling after exposure of a mixture containing 83% of K15 and cured at 25 °C leads to the formation of new deformed droplets all over the sample and to an increase of the size of the pre-existing nonspherical droplets. As in the former case, going back to the initial curing temperature reduces the sizes of droplets. Restarting the UV irradiation leads to secondary phase separation within the droplets already formed.[24]

Finally, a third series of photopolymerizations of mixtures containing low LC concentrations (between 70% and 40%) has been performed at 20 °C. The results point out that as the amount of LC in the starting mixture decreases, the phase separation process is further delayed with respect to conversion (a much higher UV dose is required before phase separation starts). Also, the size of the LC domains at incipient turbidity decreases as the LC percentage decreases. At 60% they are so small that it is impossible to say whether they are spherical or nonspherical. At 50% and 40% of K15 no phase separation is observed under the microscope anymore. However, under crossed-polarizers, some very small anisotropic patterns can be seen. They could be indicative of the presence of very small aggregates of nematic K15 in the sample or of a (shrinkage) stress in the network.

The most striking results from these series of experiments are the absence of coalescence in all but one polymerization experiment and the abrupt change of the shape of the LC domains (from spherical to nonspherical) as a function of initial LC content and curing temperature.

3.2.2. Conversion at Incipient Turbidity. Measurements have been performed on three different systems: (1) 83% K15, 17% TEGDA, cured at 20 °C; (2) 78% K15, 22% TEGDA, cured at 10 °C; (3) 78% K15, 22% TEGDA, cured at 20 °C. A typical example of a photo DSC curve together with a turbidity curve is shown in Figure 6. In the first two experiments, the fractions of double bonds which have reacted at incipient

Table 1. Microscopic Observations during Polymerization-Induced Phase Separation in TEGDA/K15

	high LC content		medium LC content	
K15/TEGDA ratio	95/5 (Figure 3)	91/9	85/15	83/17 (Figure 4)
curing temp (°C)	20 and 25	25	25	20
UV intensity (mW/cm^2)	0.2	0.1	0.3	0.3
irradiation time (s)	403	624	180	182
shape and phase of the droplets	spherical and isotropic, transforming to nematic later on	spherical and isotropic, transforming to nematic later on	spherical (slightly deformed) and nematic	spherical and nematic, deformation upon growth
coalescence during exposure	only at 20 °C, not at 25 °C	no	no	no
observations upon cooling from 25 to 20 °C at 1 °C/min	large increase of size of the isotropic droplets which become nonspherical (honeycomb-like) when their walls touch	increase of size of the isotropic droplets which become nonspherical	increase of size of the droplets which become nonspherical; formation of new deformed nematic droplets	not done
	coalescence (considerable)	coalescence (few droplets only)	no coalescence	
	I → N transition in droplets	I → N transition in droplets		
	anisotropic walls	anisotropic walls	anisotropic walls	
observations upon heating from 20 to 25 °C at 1 °C/min	walls remain in place, become isotropic; next: N → N + I transition in droplets	walls remain in place, become isotropic; next: N → N + I transition in droplets	walls remain in place, become isotropic; decrease of the size of the LC domains (starting with the small ones), followed by disappearance of most of them	not done
	isotropic walls and large isotropic LC domains at 25 °C	at 25 °C almost complete recovery of the original morphology before *T* scan, isotropic walls and isotropic LC domains	at 25 °C recovery of the original morphology before *T* scan	

	medium LC content			low LC content	
K15/TEGDA ratio	83/17 and 80/20	78/22 (Figure 5)	78/22	70/30	60/40; 50/50; 40/60
curing temp (°C)	25 25	20	10	20	20
UV intensity (mW/cm^2)	0.3	0.3	0.3	1	1
irradiation time(s)	226	248	218	>300	>300
shape and phase of the droplets	nonspherical (deformed) nematic droplets	nucleation of spherical nematic droplets which rapidly become strongly deformed upon growth	small spherical nematic droplets (nonspherical at <77% LC and 10 °C)	late phase separation of very small nematic droplets; impossible to establish their shape	no phase separation observable
coalescence during exposure	no	no	no	no	not observable
observations upon cooling from 25 to 20 °C at 1 °C/min	new deformed nematic LC domains; increase of the size of the preexisting droplets; partial homeotropic alignment of the LC; anisotropic walls	not done	not done	not done	not done
observations upon heating from 20 to 25 °C at 1 °C/min	walls become isotropic first decrease of the size of the LC domains; recovery of the original morphology (before temperature scan)	not done	not done	not done	not done

turbidity are 51% and 37%, respectively. In these two gels spherical droplets are formed. In the third experiment 72% of the double bonds have reacted at incipient turbidity. This shows up as a much later development of turbidity and a nonspherical shape of the LC domains.

3.2.3. Effect of Lowering the Cross-Link Density. At a constant LC content of 80% we have reduced the cross-link density of the model system by replacing part of the TEGDA by 2-ethoxyethyl acrylate (EEA) (**4** in Figure 1). EEA is a monoacrylate which is about half the size of a molecule of TEGDA. It was chosen since it resembles TEGDA so strongly that the overall chemical composition of the polymer hardly changes. Its solubility parameters in the monomeric and polymeric state, calculated from group contributions,[29] are almost

Figure 3. Morphology observed under crossed polarizers on cooling after polymerization at 25 °C. Composition: 81% K15, 9% TEGDA. I_{UV} = 0.3 mW/cm^2. Irradiation time: 182 s. Temperature: 20.5 °C.

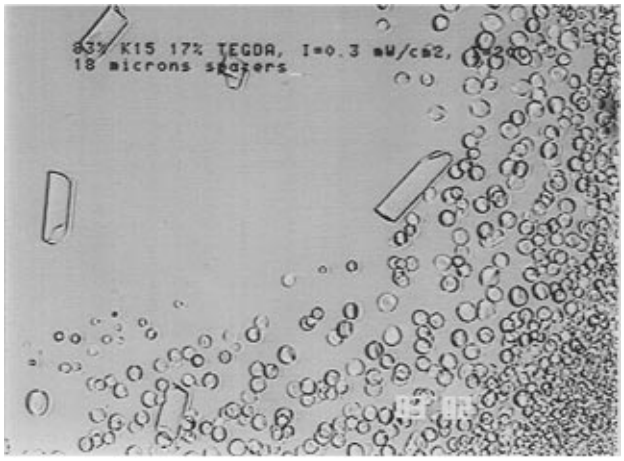

Figure 4. Spherical droplets at the onset of the phase separation. Composition: 83% K15, 17% TEGDA. Temperature: 20 °C. I_{UV} = 0.3 mW/cm^2. Irradiation time: 182 s. Straight bars are glass spacers with a thickness of 18 μm. No polarizers.

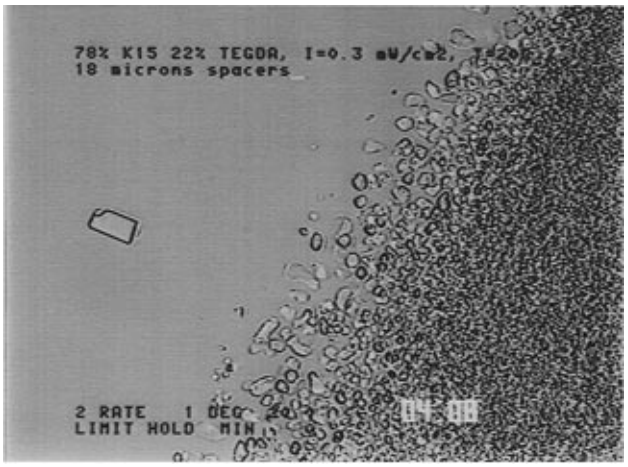

Figure 5. Nonspherical droplets at the onset of the phase separation. Composition: 78% K15, 22% TEGDA. Temperature: 20 °C. I_{UV} = 0.3 mW/cm^2. Irradiation time: 248 s. Straight bars are glass spacers with a thickness of 18 μm. No polarizers.

equal to those obtained for TEGDA and poly(TEGDA): 21.2 and 21.9 J$^{1/2}$·cm$^{3/2}$ for EEA and 21.2 and 22.0 J$^{1/2}$·cm$^{3/2}$ for TEGDA. Therefore, the intermolecular interactions in the starting mixtures and in the polymerized mixtures will be basically unchanged apart from

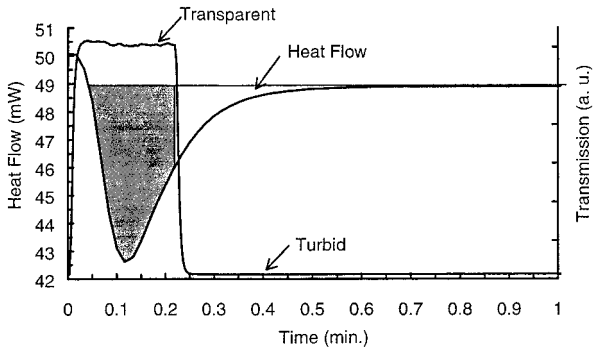

Figure 6. Photo DSC/turbidity measurement: 78% K15, 22% TEGDA, cured at 20 °C, I_{UV} = 8 mW/cm^2. The gray area represents the extent of double bond conversion at the onset of the phase separation.

the desired effect caused by the change in cross-link density. The total number of double bonds in the starting mixture also remains constant. Nevertheless, the phase diagram might change by replacing TEGDA with EEA since the number of particles changes. We did not determine phase diagrams of all mixtures studied but rather checked that the clearing points at 80% LC did not change by more than a few degrees. The clearing temperatures were 14 °C for 20% TEGDA, 9 °C for 13% TEGDA/7% EEA, and 12 °C for both 7% TEGDA/13% EEA and 20% EEA. The observed changes are rather restricted, so it can be expected that differences observed during polymerization are dominated by the large differences in cross-link density rather than by the more subtle changes caused by the interchange of the molecular species as such.

Optical microscopy during UV polymerization at 25 °C of samples containing 80% K15 and 20% of a mixture of EEA and TEGDA shows that upon lowering of the cross-linker content, the shape of the LC domains at the onset of the phase separation initially remains nonspherical (TEGDA concentration in the mixtures down to 13%, Figure 7a,b). By further reduction of the cross-linker content (down to 1% TEGDA in the mixture), the domain sizes become so small that their shape is difficult to determine (Figure 7c). Upon complete replacement of TEGDA by EEA spherical domains are formed (Figure 7d) and coalescence occurs. Moreover, as the content of EEA increases, higher UV doses are needed before phase separation sets in. These results are in agreement with photo DSC/turbidity measurements which demonstrate that the phase separation occurs at a higher double bond conversion as the cross-linker content decreases (Table 2).[23,24]

4. Discussion

4.1. Phase Diagrams. 4.1.1. Binary Phase Diagrams of Monomer and LC. Very few binary phase diagrams of liquid crystals and monomers have been reported in the literature. The phase diagram of the E7/NOA system has been reported by Smith.[19] The most precisely described system is the mixture of E8 and 2-ethylhexyl acrylate/urethane−diacrylate as prepolymer mixture, reported by Hirai et al.[13] Since E8 is composed of five different LC compounds, their system is a multicomponent system. Their pseudobinary diagram shows a liquid−liquid demixing curve with an upper critical solution temperature overlapping with the nematic−isotropic transition range of the LC rich phase. The major difference between the diagrams in Figure 2 and ref 13 is the absence in the former of a two-phase region constituted of two isotropic liquids. Hirai et al.

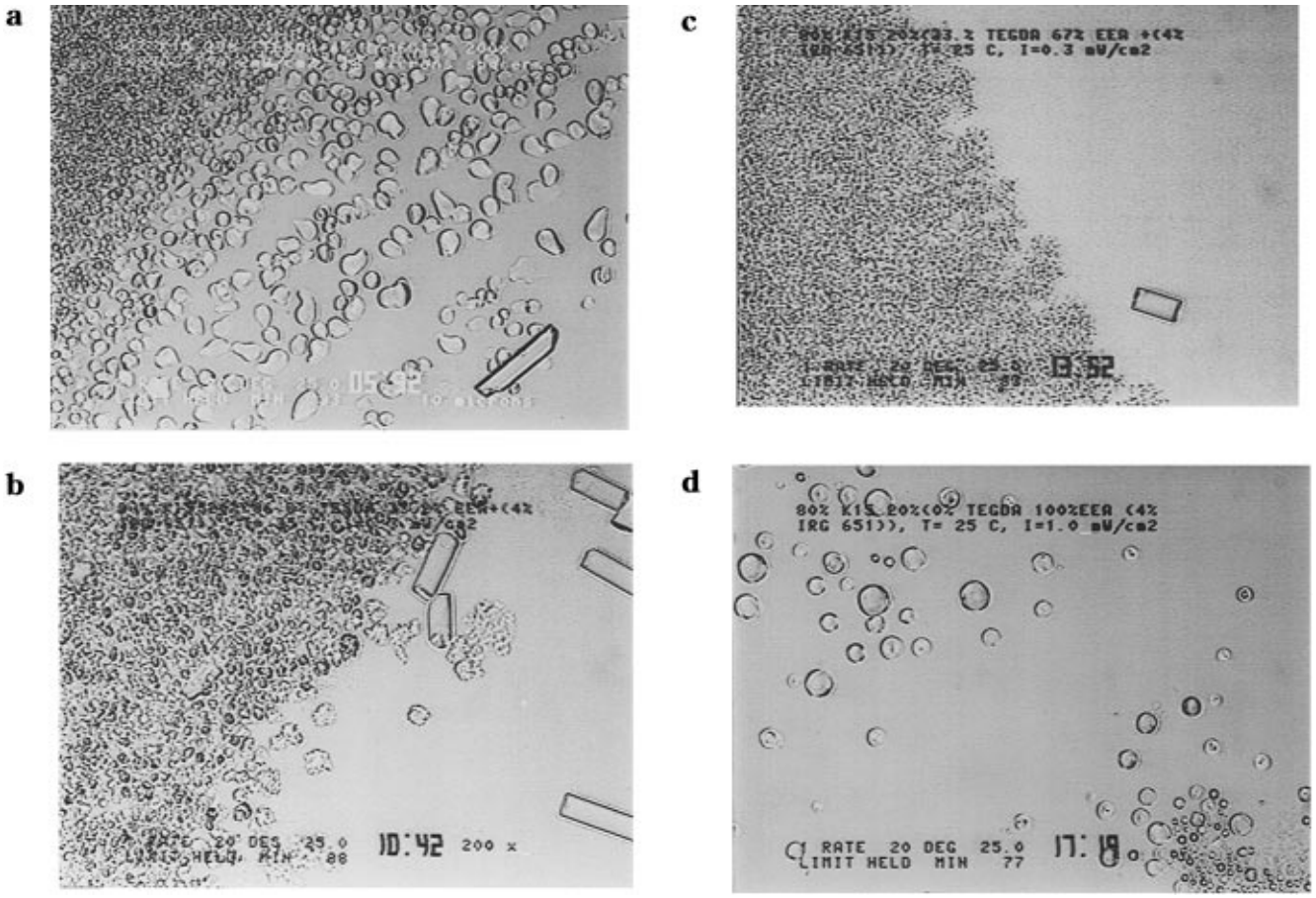

Figure 7. Morphologies of the droplets at the onset of the phase separation: (a) 80% K15, 20% TEGDA, cured at 25 °C, I_{UV} = 0.2 mW/cm^2; (b) 80% K15, 13% TEGDA, 7% EEA, cured at 25 °C, I_{UV} = 0.3 mW/cm^2; (c) 80% K15, 7% TEGDA, 13% EEA, cured at 25 °C, I_{UV} = 0.3 mW/cm^2; (d) 80% K15, 20% EEA, cured at 25 °C, I_{UV} = 1 mW/cm^2. Straight bars are glass spacers with a thickness of 18 μm. No polarizers.

Table 2. Extent of Conversion of TEGDA/EEA/K15 at Incipient Turbidity[a]

[TEGDA (w %)	[EEA] (w %)	C=C conversion (%)
20	0	56
18	2	65
16	4	76
10	10	84
5	15	90
0	20	95

[a] Assuming complete conversion of double bonds at the end of the polymerization. LC content: 80%. Temperature of polymerization: 20 °C. Light intensity: 8 mW/cm^2.

did not mention explicitly whether these two isotropic phases have indeed been observed. In the absence of the urethane−diacrylate oligomer no UCST was observed.

During polymerization the binary system is converted to a ternary one. The basis of any ternary system is formed by its three binary mixtures. Several calculated and measured phase diagrams of a liquid crystal and a linear polymer have been reported in the literature.[11,22,30] They exhibit a behavior similar to the one reported by Hirai et al.[13] It should be stressed that all of them are pseudobinary systems: their actual number of compounds is far greater than 2. They are not a good starting point for a discussion of our ternary system since TEGDA forms a cross-linked polymer.

Phase diagrams of pure liquids and cross-linked polymers differ from those of the liquid/linear polymer systems in that phase separation occurs between a swollen network and a pure liquid rather than between polymer poor and polymer rich phases.[31] However, to the best of our knowledge no phase diagram of an LC liquid and a cross-linked polymer has been published. Since the phase diagram of LC and cross-linked polymer changes continuously during cross-linking polymerization of the model system, we have not attempted to measure them either. Instead, we use the concept of a conversion−phase diagram.

4.1.2. Phase Diagrams and Polymerization: Conversion−Phase Diagrams. As explained in the Introduction and further discussed in section 4.2.1, polymerization-induced phase separation is likely to proceed through liquid−gel separation. This can be depicted in a ternary conversion−phase diagram[1] (Figure 8). The two horizontal arrows represent the polymerization of two mixtures of slightly different initial composition. At the point of intersection of such an arrow with the curved phase separation line, phase separation will start. The phase separation line can be calculated on the basis of the Flory−Huggins−Dušek theory, assuming that the cross-link density increases with the square of the double bond conversion of TEGDA and making further assumptions about the respective χ values (χ_{M-LC}, χ_{M-P}, χ_{LC-P}) and on the cross-linking efficiency. The diagram shows in a qualitative way that the extent of polymerization at which phase separation starts is very sensitive to the initial monomer or LC concentration. This is in accord with the general trend in Table 1, at both 25 and 20 °C. Upon heating, all χ values decrease so the phase separation line moves upward (Figure 9). This means that at a higher temperature liquid−gel phase separation will occur at a later stage of the chemical reaction. This is also in accord with the

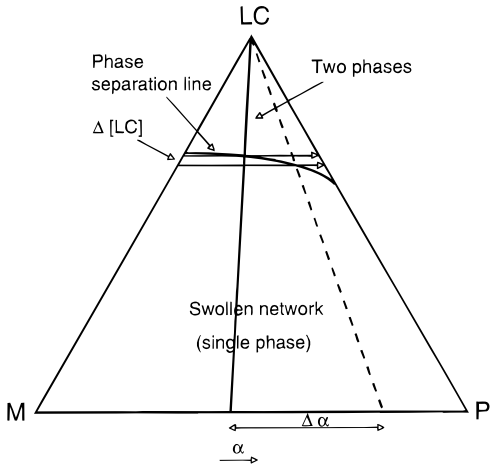

Figure 8. Ternary conversion phase diagram (schematic): effect of the initial LC concentration on the phase separation process. α: degree of monomer conversion.

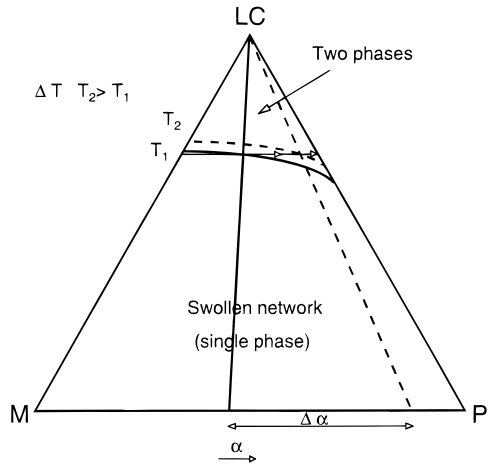

Figure 9. Ternary conversion phase diagram (schematic): effect of the temperature of polymerization on the phase separation process. α: degree of monomer conversion.

results from Table 1 (columns 78/22). Reduction of the cross-link density (through replacement of TEGDA by EEA) is equivalent to a reduction in the cross-link efficiency. Likewise, the phase separation line will be displaced vertically, causing a delay of the liquid−gel phase separation at a constant LC content (ref 1, Figure 3). This has indeed been observed (Table 2).

Cooling after polymerization will cause a lowering of the phase separation line such that the conditions for phase separation inside the saturated gel phase are met. In a loosely cross-linked gel the size of the liquid domains will increase (Table 1, High LC content); in a more densely cross-linked gel elasticity opposes the growth such that it becomes advantageous to form new small droplets, in spite of the high surface energy (Table 1, medium LC content). Depending on the strength of the gel, subsequent heating to the curing temperature may or may not lead to recovery of the orginal morphology.

4.2. Phase Separation and Morphology. The most striking observations reported in Table 1 are the absence of coalescence in all but one polymerization experiment and the abrupt change of the shape of the LC domains (from spherical to nonspherical) with decreasing LC content. Both phenomena can be explained if it is assumed that gelation occurs prior to phase separation. Other points to be commented on are the formation of an initially isotropic phase upon polymerization, the formation of anisotropic walls upon cooling and secondary phase separation.

4.2.1. Phase Separation. Isotropic Phase Formation. If phase separation proceeded through monomer depletion in the binary monomer/LC mixture a nematic phase would have to appear right at the beginning (Figure 2). Since at high LC content two isotropic phases are formed initially (Table 1), depletion-induced liquid−liquid demixing in the gel can be ruled out so the polymer must be involved in the separation process, either as a gel phase or as a polymer rich solution of microgel particles.

Absence of Coalescence. So far, we have not been able to measure gel points in thin polymerizing samples of less than 1 mg. However, from studies of the bulk polymerization of mixtures of mono- and divinyl compounds it is well-known that gelation occurs very early in the reaction, often around 1% conversion of the double bonds, and it does not strongly depend on the cross-linker content at divinyl concentrations between 10 and 100%.[32] Conversion at gelation is always much higher than what is expected from the Flory−Stockmayer theory for the very high degrees of polymerization occurring in radical reactions (DP > 10^3). This has been ascribed to intramolecular cross-linking or cyclization.[33,34] Dilution enhances cyclization and therefore further postpones gelation. Previously, we have estimated the kinetic chain length of the bulk photopolymerization of 1,6-hexanediol diacrylate (HDDA) to be 1.5 × 10^5 units per primary radical.[35] This leads to a very early gelation, at ≪1% conversion. A rough estimate for a 20% solution of TEGDA along the same lines shows that in the present case the kinetic chain length will be only of the order of 500 C═C units per primary radical at the rate maximum. In an unperturbed situation gelation would then be expected near 0.2% double bond conversion. The relevance of the primary kinetic chain length to the gel point has been explained in detail by Matsumoto in a recent review.[27] For diallyl phthalate (DAP), the most extensively studied monomer with respect to gelation, the gel point shifted from 49 to 22% conversion in going from a 33% solution to bulk monomer. At the same time the degree of polymerization went up from 20 to 33. A further increase of the degree of polymerization will cause a further decrease of the conversion at gelation. Therefore, we are pretty sure that gelation will have occurred before phase separation. In those cases where we have measured conversion at the onset of phase separation (turbidity) the conversion is always >20% and it occurs near or beyond the rate maximum so there is an ample margin of more than two decades between the theoretical gel point and the observed phase separation.

An alternative explanation for the absence of coalescence is a strong rise in viscosity. The delay of gelation is usually ascribed to the formation of microgel particles which agglomerate in a later stage to form a continuous gel.[33,34] The viscosity of microgel solutions is always much lower than that of a solution of the same concentration of a linear polymer of the same MW.[36] Suppression of coalescence by a high viscosity of the solution is therefore unlikely, the more so since, upon an increase in viscosity by cooling only 5 deg, coalescence does occur, presumably through rupture of the gel (Table 1, column 91/1).

In the case of 80% K15/20% EEA, phase separation (as determined from turbidity) sets in at a very high conversion of 95% (Table 2). So here the viscosity must also be very high. However, coalescence still occurs, in spite of the fact that the droplet density is not higher than in the case of K15/TEGDA. From this we conclude

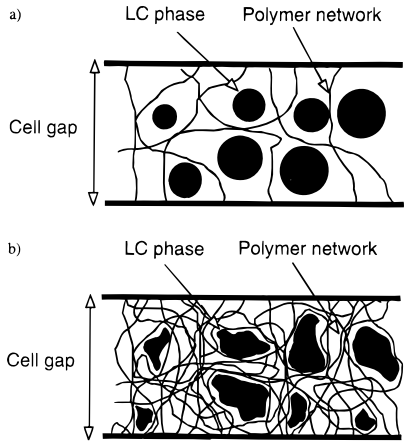

Figure 10. Schematic representation of the gel at the onset of the phase separation: (a) 83% K15, 17% TEGDA, cured at 20 °C, or 78% K15, 22% TEGDA cured at 10 °C; (b) 78% K15, 22% TEGDA, cured at 20 °C. No polarizers.

that, apart from 80% K15/20% EEA, the observed phase separations are liquid−gel demixing. In the case of 80% K15/20% EEA only size-induced and χ-induced phase separation may occur.

Secondary Phase Separation. The phenomenon of secondary phase separation has been observed by various workers.[20,21,24,38] It deserves attention in future work since it might well affect the electro-optical response of the PDLC cells.

4.2.2. Morphology. Change of Droplet Shape at Incipient Phase Separation. The transition between spherical and nonspherical upon decreasing the LC content is an unexpected phenomenon. The LC concentration where the transition from one to the other shape occurs depends on temperature: 83% LC at 25 °C, 80% at 20 °C and 77% at 10 °C.

The change in shape from spherical to nonspherical clearly reflects the inhomogeneous character of the gel. There is much experimental evidence that intramolecular cross-linking during chain cross-linking polymerization leads to inhomogeneous network structures.[34] The preparation of microporous polymers for ion exchange resins is based on this principle.[37] In a loosely cross-linked gel the elasticity is so low that the droplets can easily assume their ideal spherical shape to minimize surface interactions. In a more densely cross-linked gel the higher elasticity not only opposes the growth of the droplets, leading to a larger number of smaller droplets (Table 1, column 70/30), but also modifies the shape. Since the gel is inhomogeneously cross-linked, the elasticity also varies spatially. This causes the irregular shapes of droplets formed in systems with medium LC content (Table 1). In some cases the droplets start spherical but become deformed upon growth (Table 1, column 78/22). It might well be that all droplets start spherical but that the diameter at which they change their shape depends on the value and the spatial distribution of the cross-link density. The inhomogeneity of the gel likewise explains the change in droplet shape observed on cooling (Table 1, column 91/9).

The change in morphology with LC content is depicted schematically in Figure 10.

It is expected that the LC concentration where the transition between spherical to nonspherical occurs is a function not only of the curing temperature but also of the UV light intensity since the rate of initiation affects the (in)homogeneity of the gel. We have already found that at high intensity, phase separation (turbidity) occurs at a lower conversion than at a low light intensity.[23,24]

Conversion at Incipient Turbidity. Since there is no simple relation between conversion and cross-link density, we have no direct access to the latter. Making the oversimplified and incorrect assumption that cyclization can be neglected and that free and pendent double bonds react with the same probability, we can obtain some idea of the structure of the gel at the appearance of turbidity (Table 3). In practice, cyclization will enhance the number of doubly reacted molecules in the network, thereby decreasing the fraction of pendent bonds and increasing the fraction of free monomer. The percentages listed in Table 3 for monomer, pendent, and cross-link serve only as illustration: the actual values will certainly be quite different.

In experiments 1 and 2 the gel is only lightly cross-linked at the onset of the phase separation. In such a gel spherical droplets are formed. In experiment 3 considerably more of the monomer units have reacted at both ends, so this gel is much more cross-linked at incipient turbidity. Due to its high and inhomogeneously distributed elasticity it will impose a nonspherical shape to the LC domains. The question remains whether double bond conversion at phase separation completely determines the droplet shape. Generally, this is not the case. Experiments 3 and 4 in Table 3 show the opposing effects of increasing LC content and increasing curing temperature on the conversion at incipient phase separation. At 78% LC and 20 °C nonspherical LC domains are found, whereas at 85% LC and 25 °C spherical LC droplets are obtained. An explanation for the presence of these two different morphologies may be found in the early stage of the polymerization process. At the lower monomer content, the formation of microgel particles is enhanced since the probability of a polymeric radical to react with a pending acrylate of the same polymer chain is higher than the probability to react with another free monomer.[33,34,37] At some stage the gel is constituted of rather densely cross-linked microgel particles connected to each other by a loosely cross-linked network. Therefore, a large fraction of the cross-links are elastically inactive and a relatively high conversion of double bonds is required for phase separation. Since the elasticity of the gel remains weak, the LC phase separates as spherical droplets. In the monomer rich system a somewhat less inhomogeneous gel will be formed which has a higher elasticity at the onset of phase separation and hence the droplets will be deformed (the gel is still inhomogeneous).

Anisotropic Walls. The anisotropic walls observed on cooling can be attributed to a significant concentra-

Table 3. Double Bond Conversion at Incipient Turbidity and Hypothetical Composition of the Gel

exp. no.	composition % K15/% TEGDA	T (°C)	conversion at turbidity (%)	droplet shape	monomer (%)[a]	pendent (%)[a]	cross-link (%)[a]
1	83/17	20	51	spherical	24	50	26
2	78/22	10	37	spherical	40	46	14
3	78/22	20	72	nonspherical	8	40	52
4	85/15	25	77	spherical	5	36	59

[a] assuming no cyclization.

tion of LC molecules in the polymer walls. Cooling first leads to deswelling and expulsion of LC molecules from the gel so that the size and the purity of the droplets increase. By the combined processes of cooling and purification the droplets become nematic. At a still lower temperature the rate of nucleation increases and a large number of very small, microscopically unresolved nematic domains separate out.

4.2.3. Mechanism of Liquid−Gel Phase Separation. The mechanism of phase separation, spinodal decomposition, or nucleation and growth, is the subject of an ongoing discussion. Recently, spinodal decomposition has been advocated,[20,21,38] but nucleation and growth has also been proposed.[9] In the latter case the minor phase is expected to separate out as droplets in the major phase.[39]

In section 4.2.1, we have concluded that liquid−gel separation rather than liquid−liquid separation occurs during photopolymerization of the model system. In principle, both processes may proceed through binodal or spinodal decomposition,[34] the depth of quench being the decisive parameter. The depth of quench is well-defined for thermally induced phase separation but its meaning is less straightforward with respect to isothermal cross-linking polymerization since the phase diagram itself changes continuously with conversion. The conversion−phase diagram has no meaning beyond the phase separation line.[1] Therefore, it is difficult to arrive at a firm and final conclusion with respect to the mechanism, the more so since many phenomena may proceed prior to observation due to the limited resolution of the microscope. However, in spinodal decomposition the experimentally observed droplets should be formed by the breaking up of at least one of the two initially cocontinuous phases. In gelled systems only the liquid phase is capable of doing so, the cross-linked gel may merely coarsen its structure while remaining continuous. (Only in very weak gels might rupture occur, cf. the coalescence on cooling, Table 1, column 91/9.) Coarsening without rupture requires that the distance between cross-links exceeds the characteristic wavelength of the spinodal decomposition process. In view of the high cross-link density of poly(TEGDA) the possible spinodal periods will certainly be well below the resolution of an optical microscope. From the fact that in most cases the LC droplets are nematic (i.e. very pure) right from their appearance under the microscope and that neither their sizes nor their mutual distances show any regularity we conclude that a nucleation and growth process is more likely than spinodal decomposition, the more so since at medium LC content domains may appear and disappear in an entirely reversible way during cooling and heating after full polymerization (Table 1).

5. Conclusions

The isothermal phase separation during chain cross-linking polymerization of TEGDA/K15 is driven by liquid−gel demixing rather than by liquid−liquid demixing of the binary monomer−LC system. The abrupt change from spherical to nonspherical droplet shapes upon lowering the LC content or increasing the temperature of reaction reflects the inhomogeneity of the cross-linked gel. The influence of variation of LC content, temperature of reaction, and cross-linker content of the monomer fraction on the shape of the droplets can be explained qualitatively by means of a conversion−phase diagram calculated on the basis of the Flory−Huggins−Dušek theory. It is made plausible that the observable part of the demixing process proceeds through binodal decomposition but spinodal decomposition cannot be ruled out at a very early, submicroscopic stage.

Acknowledgment. C.S. thanks the EU for financial support of this work under contract ERB4001GT930175.

References and Notes

(1) Part 1: Boots, H. M. J.; Kloosterboer, J. G.; Serbutoviez, C.; Touwslager, F. J. *Macromolecules* **1996**, 29, 7683 (preceding article in this issue).
(2) Drzaic, P. S. *Liquid Crystal Dispersions* ; World Scientific: Singapore 1995.
(3) Doane, J. W. In *Liquid Crystals: Applications and Uses*; Bahadur, B., Ed.; World Scientific: Singapore, 1990; Chapter 14, p 361.
(4) Montgomery, G. P.; Smith, G. W.; Vaz, N. A. In *Liquid Crystalline and Mesomorphic Polymers*; Shibaev, V. P., Lam, L., Eds.; Springer: New York, 1994; Chapter 5, p 149.
(5) Doane, J. W.; Golemme, A.; West, J. L.; Whitehead, J. R.; Wu, B. G. *Mol. Cryst. Liq. Cryst.* **1988**, *165*, 511.
(6) Lackner, A. M.; Margerum, J. D.; Ramos, E.; Lim, K.-C. *Proc. SPIE−Int. Soc. Opt. Eng.* **1989**, *1080*, 53.
(7) Margerum, J. D.; Lackner, A. M.; Erdmann, J. H.; Sherman, E. *Proc. SPIE−Int. Soc. Opt. Eng.* **1991**, *1455*, 27.
(8) Drzaic, P. S. *Liq. Cryst.* **1988**, *3*, 1543.
(9) Yamagishi, F. G.; Miller, L. J.; Van Ast, C. I. *Proc. SPIE−Int. Soc. Opt. Eng.* **1989**, *1080*, 24.
(10) Smith, G. W. *Mol. Cryst. Liq. Cryst.* **1991**, *196*, 89.
(11) West, J. L. *Mol. Cryst. Liq. Cryst.* **1988**, *157*, 427.
(12) Lovinger, A. J.; Amundson, K. R.; Davis, D. D. *Chem. Mater.* **1994**, *6*, 1726.
(13) Hirai, Y.; Niiyama, S.; Kumai, H.; Gunjima, T. *Proc. SPIE−Int. Soc. Opt. Eng.* **1990**, *1257*, 2; *Rep. Res. Lab., Asahi Glass Co., Ltd.* **1990**, *40*, 285.
(14) Carter, S. A.; LeGrange, J. D.; White, W.; Wiltzius, P. *MRS Spring Meeting* **1996**, Abstr. I 4.3.
(15) Nazarenko, V. G.; Sarala, S.; Madhusudana, N. V. *Jpn. J. Appl. Phys.* **1994**, *33*, 2641.
(16) Nolan, P.; Tillin, M.; Coates, D. *Mol. Cryst. Liq. Cryst. Lett.* **1992**, *8 (6)*,129.
(17) LeGrange, J. D.; Miller, T. M.; Wiltzius, P.; Amundson, K. R.; Boo J.; Van Blaaderen A.; Srinivasarao, M.; Kmetz, A. *SID95 Digest* **1995**, *18.3*, 275.
(18) Serbutoviez, C.; Kloosterboer, J. G.; Boots, H. M. J.; Touwslager, F. J. *Liq. Cryst.*, in press.
(19) Smith, G. W. *Int. J. Mod. Phys. B* **1993**, *7*, 4187.
(20) Kim, J. Y.; Palffy-Muhoray, P. *Mol. Cryst. Liq. Cryst.* **1991**, *203*, 93.
(21) Kim, J. Y.; Cho, C. H.; Palffy-Muhoray, P.; Mustafa, M.; Kyu, T. *Phys. Rev. Lett.* **1993**, *71*, 2232.
(22) Shen, C.; Kyu, T. *J. Chem. Phys.* **1995**, *102*, 556.
(23) Kloosterboer, H.; Serbutoviez, C.; Boots, H.; Touwslager, F. *Polym. Mater. Sci. Eng.* **1996**, *74*, 190.
(24) Kloosterboer, J. G.; Serbutoviez, C.; Boots, H. M. J.; Touwslager, F. J. *Polym. Commun.*, in press.
(25) Kloosterboer, J. G. *Adv Polym. Sci.* **1988**, *84*, 1.
(26) Kloosterboer, J. G.; Lijten, G. F. C. M. In *Cross-Linked Polymers. Chemistry, Properties and Applications*; Dickie, R. A., Labana S. S., Bauer R. S., Eds.; ACS Symposium Series 367; American Chemical Society: Washington, DC, 1988; p 409.
(27) Matsumoto, A. *Adv. Polym. Sci.* **1995**, *123*, 41.
(28) Bowman, C. N.; Peppas, N. A. *Macromolecules* **1991**, *24*, 1914.
(29) Van Krevelen, D. W. *Properties of Polymers*, 3rd ed.; Elsevier: Amsterdam, 1990; Chapter 7.
(30) Kim, W. K.; Kyu, T. *Mol. Cryst. Liq. Cryst.* **1994**, *250*, 131.
(31) Rehage, G. *Kolloid Z. Z. Polym.* **1964**, *194*, 16.
(32) Malinsky, J.; Klaban, J.; Dušek, K. *J. Macromol. Sci., Chem.* **1971**, *A5*, 1071.
(33) Dušek, K.; Galina, H.; Mikeš J. *Polym. Bull.* **1980**, *3*, 19.
(34) Dušek, K. In *Developments in Polymerisation-3;* Haward, R. N., Ed.; Applied Science Publishers: London, 1982; Vol. 3, Chapter 4, p 143.
(35) Kloosterboer, J. G.; Lijten, G. F. C. M.; Zegers, C. P. G. *Polym. Mater. Sci. Eng.* **1989**, *60*, 122.
(36) Whitney, R. S.; Burchard, W. *Makromol. Chem.* **1980**, *181*, 169.
(37) Funke, W. *Plast. Rubber Process. Applic.* **1982**, *3*, 243.
(38) Srinivasarao, M.; Amundsen, K. *Polym. Prepr. (Am. Chem. Soc., Div. Polym. Chem.)* **1996**, *37* (1), 200.
(39) Smith, G. W. *Mol. Cryst. Liq. Cryst.* **1993**, *225*, 113.

MA960293+